Analysis of the Thermal Damage on Homogenized Multi-Materials under Thermo-Mechanical Behavior

BILAL TAHER, SAID ABBOUDI
Systems and Transport Laboratory (SET)
University of Technology of Belfort-Montbeliard
Site of Sevenans, 91000, Belfort Cedex
FRANCE
{bilal.taher, said.abboudi}@utbm.fr

RAFIC YOUNES
Associate professor
Quebec University
Rimouski
CANADA
rafic_younes@uqar.qc.ca

Abstract: - In the recent high technologies, the increasing need of structures having multiple functions orientates designers to combine materials in order to obtain, according to coupling scales, multi-materials structures. These structures, while functioning, are subject to variable thermal load, leading to a damage that can be fatal in some applications.

So, the study of the behavior of these structures, while they are under thermal cycling solicitations, seems to be very important in order to be able to predict their lifetime and their response to any applied solicitation. It is obvious that the variation of the nature of thermal and mechanical solicitation in term of amplitude and frequency leads to a variation of the resulting damage. But at the level of our knowledge, this effect is not studied before in the literature on multi-materials.

In this work, we propose a numerical analysis of the thermo-elasto-plastic behavior of these multi-materials and their damage under thermal cyclic solicitations, while using the homogenization technique. This study is done in two dimensions on a cylindrical multi-material constituted of two layers, subjected to a periodic heat flux applied in the inner face of this cylinder and an exchange condition on the opposite face. The other faces are supposed isolated. The sample is supposed fixed at the isolated faces and free in the radial direction. The damage model is based on the works of Lemaitre and Chaboche [6]. This damage model is not done for multi-materials; it is applicable only to one material apart. So the homogenization of these multi-materials permits us to study the damage of the multi-layers as it is a unique material.

The numerical results are presented for different forms and frequency of heat flux cycling (triangular, square and sinusoidal wave excitations) and for different thicknesses of the multi-material. Finally we do a comparison of the multi-material damage with respect to different heat flux excitations.

Key-Words: - Thermal stress, thermo-mechanical, damage, thermo-elasto-plastic, coupling, multi-material, cycling, thermal load.

1 Introduction

The study of metallic components solicited with high temperatures has really started in fifties by the aeronautic industry first, then with the beginning of the nuclear industry. These materials have been submitted to very high temperatures, sometimes more than half the temperature of fusion. In this range of temperatures, their mechanical properties are considerably modified and / or the damage mechanisms are multiplied. The solicitations cycles, to which these metallic structures are submitted, frequently cause cyclic inelastic deformations. Every system or mechanical component is likely to be subject to a thermo-elasto-plastic coupling. This is due to the fact that the abrupt variation and the periodicity of the temperature influence the fatigue of constituent materials. This consequently leads to the complete destruction of the materials.

The presence of thermal and mechanical loads in every system motivates the researchers to work in this domain and especially in the field of variable load and its influence, by means of period solicitation, amplitude and shape, on the material damage, [1], [2], [3], [4], [5].

Almost all previous works address only the effect of mechanical load on the damage. We can find experimental studies as well as studies done by means of simulation and modeling [6], [8], [3], [9].

[1], [4], conducted a study by the use of very high frequency mechanical vibration. They concluded that there is a relationship between the load frequency and the fatigue of the material under mechanical solicitation. They proved also that there is a fatigue variation relative to the material resonance value. Based on the above studies, it is very important to study the influence of the frequency variation and the thermal load amplitude on the lifetime and on the number of cycles to damage.

This does not mean that the thermo-mechanical effect was not studied before. There are some advanced studies that analyze the thermo-mechanical damage under thermal load, but their studies are still limited by the assumption that the thermal load is constant [10], [11]. The mechanical load is considered as variable. This assumption is taken in order to simplify the study by neglecting the transient regime of the thermal load. In general, these approaches underestimate the thermo-elasto-plastic behavior of these materials and as a result their behavior in fatigue [11].

Some other studies take into consideration the transient regime of a variable thermal load, but these are experimental studies only and are not done by means of physical models [14]. In fact, there is an important difficulty in the finding of the correct damage model, because there is no damage law that takes into consideration a variable thermal load. This is verified by the presence of a lot of mechanical damage laws in the literature, but of only one law for isothermal damage [6]. At the level of our knowledge, there is not a variable thermal damage law that can be used in thermo-mechanical damage modeling.

From another point of view, the experimental works that study the effect of variable thermal load on the damage, and in order to show the effect of the frequency of this thermal load, consider only a limited number of values for the frequency, and cannot extend their studies to all frequency ranges because this will be more and more expensive to experiment with. [14], [10].

Also, in the literature, there are no thermo-mechanical damage studies on multi-materials. In fact, for the damage study, the existing laws of damage, in the scientific field, especially those by [7], [6] cannot be applied on multi-materials; they can only be applied on simple and unique materials.

Furthermore, the studies of both layers, supposed to be in perfect contact, lead to perfect theoretical results; for example, they lead to an ideal heat transfer and the stress is distributed regularly and is discontinuous at the level of the interface between layers.

It is also evident that in a two-layer material, there is a mutual influence of one material on the other; we cannot have an abrupt variation of the thermal and mechanical properties at the level of the joint. At this level, we have a certain region in which the values of thermal and mechanical properties are supposed to vary between those of the constituting materials. This reasoning imposes the necessity of searching for a method of correction based on the principle of homogenization of multi-materials in a single equivalent material. This latter has to undergo the study of the damage under thermo-mechanical stress [14], [15].

The homogenization approach proposed in [13] replaces the multi-material with a unique material having constant and equivalent thermo-physical properties obtained by means of models that allow us to have similar temperatures in both materials and in equivalent materials as well.

This approach cannot be used to obtain the correct value of the damage in each point of the material because in reality the temperature cannot be constant and similar in all points. For this reason, we use herein the homogenization approach detailed in [15] which replaces the two materials with a unique one where the proprieties vary with the geometry. This technique is validated in this work and gives good results.

After this introduction, a set of abbreviations and symbols used in this paper are presented in section 2. A description of the sample studied is detailed in section 3. The mathematical formulation of the thermal mechanical problem, coupling and damage is shown in section 4. In section 5, we carry out a numerical analysis of the problem. The conclusion of this paper is given in section 6.

2 Nomenclature

Symbols:

B_0 constant of the damage law MPa

C calorific capacity, $J/Kg.K$

D number of cycles to damage

E Elasticity modulus, Pa

e_i thickness of the layer $i = 1, 2$

e thickness of the body $e = e_1 + e_2$

h coefficient of convection, $W/m^2.K$

K_y coefficient of plastic resistivity *MPa*

L length *m*

LFT   lifetime *S*

M_y exponent of work hardening

Q heat flux density, W/m^2

r radial coordinate, *m*

$\overset{\bullet}{r}$ heat source W/m^3

T temperature, *K*

T_0 initial temperature, *K*

T_a ambient temperature, *K*

U displacement according to *r, m*

V displacement according to *z, m*

z axial coordinate, *m*

Greek letters:

α expansion coefficient, *m/K*

β exponent of the damage law

ρ density, Kg/m^3

λ thermal conductivity, *W/m.K*

ν poison coefficient

σ stress tensor, *Pa*

$\overline{\sigma}$ average stress tensor, *Pa*

σ_l limit stress tensor, *Pa*

σ_M maximum stress tensor, *Pa*

σ_s stress tensor, *Pa*

σ_u ultimate stress tensor, *Pa*

σ_y elastic limit stress, *Pa*

ε deformation tensor

ε^e elastic deformation tensor

ε^p plastic deformation tensor

ε^{th} thermal deformation tensor

ε^c creep deformation tensor

τ period, *s*

3 Presentation of the problem

The body studied is constituted of two layers of different materials, the sub-base "Material-1" is a layer made of stainless steel and the other "Material-2" is made of Steel (see Fig. 1). The physical specifications of these two materials are presented in Table 1.

The internal surface of the sample is submitted to a periodic heat flux and the external surface is submitted to a heat transfer by convection with the ambient. The left and right sides are supposed to be insulated.
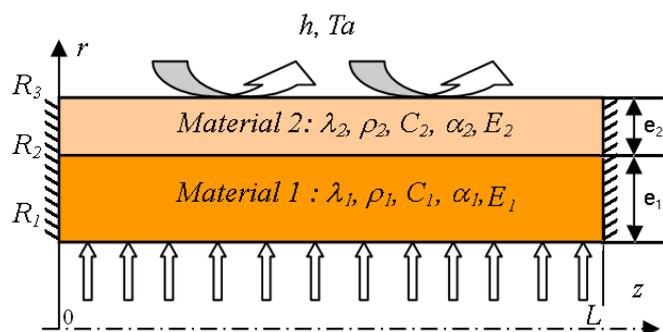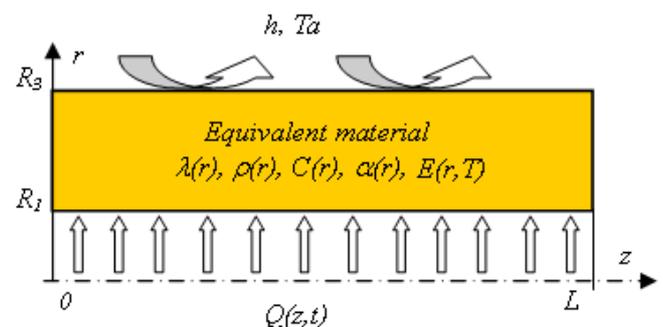

Fig. 1: The studied sample

The equivalent material of the system described above is obtained by using a polynomial interpolation of the physical parameters $\phi = (\rho, c, \lambda, \alpha, E(T))$, Fig. 2:

$$\phi(r) = \sum_{k=0}^{n} a_k r^k \qquad (1)$$

	Stainless steel	Steel
ρ: density	7854 kg/m3	7854 kg/m3
c: heat capacity	477 J/Kg.°K	434 J/Kg.°K
λ: thermal conductivity	35 W/m°K	60.5 W/m°K
α: expansion coefficient	15.10-6 m/K	11.8.10-6 m/K
ν: poison coefficient	0.3	0.3
L: length	0.6 m	0.6 m
R1: internal radius	0.1 m	0.1 m
e: thickness	e1 = 0.03 m	e2 = 0.03 m

Table 1: Physical specifications of materials [17]

Note here that this study is applicable to any material having variable physical parameters. So, it is not important here to identify the material presented in Fig. 2 and to specify the materials from which it is generated. The essential thing to keep in mind is that we have a material having variable physical parameters according to r.

Fig. 2: Equivalent Material

4 Mathematical formulation

Our approach consists of considering the thermal equation while taking into account the presence of heat created by the elasto-plastic behavior of the material and caused by the external thermal solicitation. This thermal equation helps us to observe the evolution of the distribution of the temperature and then the thermal behavior of the body with respect to the thermal excitation applied to it. Then the thermo-elasto-plastic problem is considered to observe the evolution of the distributions of the deformations of the body and then the thermo-mechanical behavior of the material.

In the following paragraph, the mathematical formulations are presented respectively for both the multi-material and the equivalent material. The contact between the two layers is considered to be perfect.

4.1 Thermal Formulation

In the thermo-mechanical coupling system, the transient heat transfer balance equation [6], [18], [19], [20] is:

$$\rho C \dot{T} = div(\lambda \, \overrightarrow{grad} \, T) + \sigma : \dot{\varepsilon}^p - A_k \dot{V}_k + \overset{\bullet}{r}$$
$$+ T\left[\frac{\partial \sigma}{\partial T} : \dot{\varepsilon}^e + \frac{\partial A_k}{\partial T} \dot{V}_k \right] \quad (2)$$

Where:

$div(\lambda \, \overrightarrow{grad} \, T)$ is the adiabatic evolution, $A_k \dot{V}_k$ is the non-recoverable energy stored in the material,

$\sigma : \dot{\varepsilon}^p$ is the plastic energy, $T\dfrac{\partial \sigma}{\partial T} : \dot{\varepsilon}^e$ is the energy

of thermo-mechanical coupling, $T\dfrac{\partial A_k}{\partial T} \dot{V}_k$ is the

variation of the non-recoverable energy stored in the material with the temperature.

And finally $\overset{\bullet}{r}$ is the internal heat production created by external sources.

In this work, the following hypotheses are supposed:

- The internal heat generation is neglected $\overset{\bullet}{r} = 0$.
- The energy belongs to the residual micro-stress field accompanying the increase of the dislocation density [6] represents only 5 to 10 % of the value of $\sigma : \dot{\varepsilon}^p$. Then this energy is neglected,

$$A_k \dot{V}_k \cong 0 \text{ and } T\frac{\partial A_k}{\partial T} \dot{V}_k \cong 0 \quad (3)$$

4.1.1 Theoretical materials

Under these hypotheses, the theoretical thermal model of the studied system is:

$$(\rho C)_i \cdot \frac{\partial T_i}{\partial t} = \lambda_i \left(\frac{1}{r}\frac{\partial}{\partial r}\left(r\frac{\partial T_i}{\partial r}\right) + \frac{\partial^2 T_i}{\partial z^2}\right), i = 1, 2 \quad (4)$$
$$+ T_i \frac{\partial \sigma_i}{\partial T} : \frac{\partial \varepsilon_i^e}{\partial t} + \sigma_i : \frac{\partial \varepsilon_i^p}{\partial t}$$

With: $i = 1$ (stainless steel), $i = 2$ (Steel)

The boundary conditions and the heat transfer equations applied to the boundaries can be written as follows:

$$-\lambda_1 \frac{\partial T}{\partial r} = \phi(z,t) \qquad r = R_1 \quad 0 < z < L \quad (5)$$

$$-\lambda_2 \frac{\partial T}{\partial r} = h(T - T_f) \qquad r = R_3 \quad (6)$$

$$-\lambda_i \frac{\partial T}{\partial z}\bigg|_{z=0} = -\lambda_i \frac{\partial T}{\partial z}\bigg|_{z=L} = 0, \; i = 1, 2 \quad (7)$$

Interface conditions:

$$-\lambda_1 \frac{\partial T}{\partial r} = -\lambda_2 \frac{\partial T}{\partial r}, \qquad r = R_2 \quad (8)$$

- Initial condition: $T(r,z,0) = T_0$

4.1.2 Homogeneous material

For the homogeneous material, the thermal equation is as follows:

$$(\rho C)(r)\frac{\partial T}{\partial t} = \left(\frac{1}{r}\frac{\partial}{\partial r}\left(r\lambda(r)\frac{\partial T}{\partial r}\right) + \lambda(r)\frac{\partial^2 T}{\partial z^2}\right).$$
$$+ T\frac{\partial \sigma}{\partial T} : \frac{\partial \varepsilon^e}{\partial t} + \sigma : \frac{\partial \varepsilon^p}{\partial t} \quad (9)$$

Where T, σ, ε^e and ε^p are functions of (r,z,t)

The boundary conditions can be written as follows:

$$-\lambda(r)\frac{\partial T}{\partial r} = \phi(z,t) \qquad r = R_1, \; 0 < z < L \quad (10)$$

$$-\lambda(r)\frac{\partial T}{\partial r} = h(T - T_0) \qquad r = R_3 \quad (11)$$

$$-\lambda(r)\frac{\partial T}{\partial z}\bigg|_{z=0} = -\lambda(r)\frac{\partial T}{\partial z}\bigg|_{z=L} = 0, R_1 < r < R_3 \quad (12)$$

- Initial condition: $T(r,z,0) = T_0$

4.2 Thermo-mechanical equation in elastic regime

The thermo-mechanical equation in the elastic regime is obtained by the introduction of the thermal deformation in the Lame mechanical behavior equation [18], [19].

$$\sigma(r,z,t)_{ij} = E(T)_{ij}(\varepsilon_{ij} - \alpha_{ij}(T(r,z,t) - T_0)) \quad (13)$$

-Hypotheses

The stress is supposed to be unidirectional: the body is fixed in the z direction and we have $L/R = 6 << 45$. So, we have no flexion and the

maximum of the stress is applied in the fixed (isolated) sides, $z = 0$, $z = L$.

The variation of the Young modulus E is presented in Table 2.

Temperature (^{0}C)	20	205	430	650
Stainless steel (MPa)	196	183	165	146
Steel (MPa)	210	198	180	155

Table 2: Young module E variation with the temperature [26]

4.2.1   Theoretical materials

In a matrix form, for axis-symmetric isotropic material, $\alpha_{rr} = \alpha_{zz} = \alpha$ and $\alpha_{rz} = 0$

$$
\begin{bmatrix} \sigma_{rr} \\ \sigma_{zz} \\ \sigma_{rz} \end{bmatrix}_i = \left(\frac{E}{(1+v)(1-2v)} \right)_i \begin{bmatrix} 1-v & v & 0 \\ v & 1-v & 0 \\ 0 & 0 & \frac{1-2v}{2} \end{bmatrix}_i
$$

$$
\times \begin{bmatrix} \varepsilon_{rr}^e - \alpha(T-T_0) \\ \varepsilon_{zz}^e - \alpha(T-T_0) \\ \varepsilon_{rz}^e \end{bmatrix}_i, i = 1,2 \qquad (14)
$$

4.2.2   Homogeneous material

For an isotropic material in 2D, $\alpha_{rr} = \alpha_{zz} = \alpha$ and $\alpha_{rz} = 0$

For the homogenous material, we can use eq. (14) as the thermo-elastic behavior equation but without the subscript i and where v, α are functions of *(r)*, and E is function of *(r,T)*.

4. 3 Mechanical plastic Formulation

In the plasticity regime, the deformation of the material is formulated by the Ramberg-Osgood equation [6]:

$$
\varepsilon^p = \left\langle \frac{\sigma_s - \sigma_y}{K_y} \right\rangle^{M_y} \qquad (15)
$$

Where σ_s is the stress applied, σ_y is the elasticity limit stress, K_y is the plastic resistance coefficient, M_y is the hardening exponent. These parameters are defined in Table 3.

- Hypotheses

The body is fixed in the z direction: $\varepsilon_{zz}^p = 0$.

The applied stress σ_s is equal to σ_{zz} in our case.

[1] Material	[2] σ_y (MPa)	[3] M_y	[4] K_y (MPa)
[5] Stainless steel	[6] 133	[7] 4.5	[8] 435
[9] steel	[10] 1200	[11] 3.1	[12] 3340

Table 3: Plasticity characteristics [6]

4.3.1   Theoretical materials

The plastic deformations of the double-layer material are written, considering that:

- each layer is separated from the other one
- the intermediate deformations are equal $\varepsilon_{rr1}^p = \varepsilon_{rr2}^p$ $\varepsilon_{zz1}^p = \varepsilon_{zz2}^p$,
- and the decomposition of the two-dimensional plastic deformation, according to the isotropic criteria, is written as follows:

$$
\begin{bmatrix} \varepsilon_{rr} \\ \varepsilon_{zz} \end{bmatrix}_i^p = \begin{bmatrix} \left(\frac{\sigma_{zz} - \sigma_y}{K_y} \right)^{M_y} \\ 0 \end{bmatrix}_i, i = 1, 2 \qquad (16)
$$

The parameters $\sigma_{yi}, K_{yi} M_{yi}$, depend on the nature of the material, $i = 1$ (stainless Steel), $i = 2$ (Steel)

4.3.2   Homogeneous material

Using the homogeneous principle, the plastic deformation, in this case, can be written by the same expression, eq. (16), where the parameters σ_y, K_y, M_y are interpolated as a function of r.

4.4 Thermo- elasto-plastic equation

When the material runs over the elastic region, we can say that this material is in the inelastic phase, so the stress applied to the model is [17]:

$$
\sigma_{ii} = \frac{E_{ii}}{(1+v_{ii})(1-2v_{ii})} \left[(1-v_{ii})\varepsilon_{ii} + v_{ii}(\varepsilon_{jj} + \varepsilon_{kk}) \right]
$$

$$
- \frac{E_{ii}}{1-2v_{ii}} \varepsilon_{ii}^{th} - \frac{E_{ii}}{1+v_{ii}}(\varepsilon_{ii}^P + \varepsilon_{ii}^c) \qquad (17)
$$

Where i represents r, θ or z.

$\varepsilon_{ii} = \varepsilon_{ii}^e + \varepsilon_{ii}^p + \varepsilon_{ii}^c + \varepsilon_{ii}^{th}$: is the global deformation.

ε_{ii}^e is the elastic deformation.

ε_{ii}^p is the plastic deformation.

ε_{ii}^c is the creep deformation

$\varepsilon_{ii}^{th} = \alpha_{ii}\Delta T(r,z,t)$: is the thermal deformation.

Taking into account the previsions hypotheses, we can conclude that: $\varepsilon_{ii}^c = 0$

The study is two-dimensional, so,

$\varepsilon_{\theta\theta} = \varepsilon_{\theta\theta}^e = \varepsilon_{\theta\theta}^p = \varepsilon_{\theta\theta}^{th} = 0$.

The two sides of the body are fixed in the z direction, so, $\varepsilon_{zz} = \varepsilon_{zz}^e = \varepsilon_{zz}^p = \varepsilon_{zz}^{th} = 0$.

The radial deformation is $\varepsilon_{rr} = \varepsilon_{rr}^e + \varepsilon_{rr}^p + \varepsilon_{rr}^{th}$.

4.4.1 Theoretical materials

In matrix form and for a 2D isotropic material,

$$\begin{bmatrix} \sigma_{rr} \\ \sigma_{zz} \end{bmatrix}_i = \left(\frac{E}{(1+v)(1-2v)} \right)_i \begin{bmatrix} 1-v & v \\ v & 1-v \end{bmatrix}_i \begin{bmatrix} \varepsilon_{rr} \\ 0 \end{bmatrix}_i, i=1,2 \quad (18)$$
$$- \left(\frac{E}{1-2v} \right)_i \begin{bmatrix} \alpha_{rr}(T-T_l) \\ \alpha_{zz}(T-T_l) \end{bmatrix}_i - \left(\frac{E}{1+v} \right)_i \begin{bmatrix} \varepsilon_{rr}^P \\ 0 \end{bmatrix}_i$$

Where σ, ε, T are functions of (r,z,t).

4.4.2 Homogeneous material

For the homogenous material, we can use eq. 18 as the thermo-elasto-plastic behavior equation but without the subscript i and where v, α are functions of r, and E is function of (r,T).

4.5 Damage model

The Woehler-Miner law [6] is adopted in this study. The field of validity of this law is mainly the fatigue of the material under periodic solicitations. Woehler-Miner curves represent the relation existing between the number of cycles to the rupture, the maximum value of the stress σ_M and its average value $\overline{\sigma}$.

This law is convenient in our case study. In fact, the mechanical load obtained from the applied thermal solicitations is periodical and the stress applied is only function of r. Hence, the general formula for this law is:

$$\frac{\delta D}{\delta N} = \frac{\sigma_M - \sigma_l(\overline{\sigma})}{\sigma_u - \sigma_M} \left(\frac{\sigma_M - \overline{\sigma}}{B(\overline{\sigma})} \right)^{\beta} \quad (19)$$

Where:

$$\sigma_l(\overline{\sigma}) = \overline{\sigma} + \sigma_{l_0} \left(1 - \frac{\overline{\sigma}}{\sigma_u} \right) \quad (20)$$

$$B(\overline{\sigma}) = B_0 \left(1 - \frac{\overline{\sigma}}{\sigma_u} \right) \quad (21)$$

Where σ_u, σ_l, B_0, β are defined in Table 4 for the two materials :

Material	σ_u MPa	σ_l MPa	B0 MPa	β
Stainless steel	200	650	1144	5.5
Steel	360	2005	6320	3.3

Table 4: Coefficients of the damage law [6]

4.5.1 Theoretical materials

$$\frac{\delta D}{\delta N} = \frac{\sigma_M - \sigma_l(\overline{\sigma})_i}{\sigma_{ui} - \sigma_M} \left(\frac{\sigma_M - \overline{\sigma}}{B(\overline{\sigma})_i} \right)^{\beta_i}, i=1,2 \quad (22)$$

4.5.2 Homogeneous material

$$\frac{\delta D}{\delta N} = \frac{\sigma_M - \sigma_l(\overline{\sigma})}{\sigma_u - \sigma_M} \left(\frac{\sigma_M - \overline{\sigma}}{B(\overline{\sigma})} \right)^{\beta} \quad (23)$$

With σ_u, σ_l, B0, β are functions of r in the homogenous approach [15].

5 Numerical analysis

5.1 Organization of numerical Analysis

The heat balance equations systems described above for the theoretical and the homogenous materials are solved by the implicit finite difference method. At each cycle, the resulting algebraic system is solved by using Thomas algorithm adapted to the three-diagonal bloc matrix. The distribution of the temperature is computed each time and used in the mechanical problem to compute the distribution of the stress and the deformation in the body in elastic regime, elasto-plastic regime and then the damage following the organization chart:
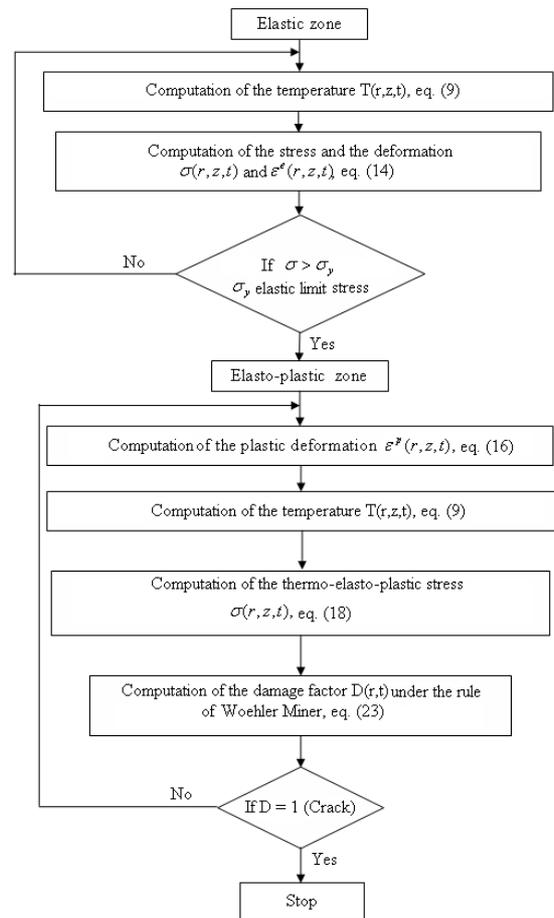

Fig. 3: Organizational chart

The numerical study is conducted in the conditions cited in tables 1, 2, 3 and 4 and the following boundary conditions:

For the thermal problem, we suppose:

$T_0 = 300\ K$, $T_a = 300\ K$, $h = 100\ W\ /(\ m^2 .K\ )$

The heat fluxes studied are presented in Fig. 4, for the following three cases which represent different industrial applications (for example turbine reactor and cylindrical engine):

Sinusoidal heat flux:

$$Q(z,t) = f(z)\left(1 + \sin\left(\frac{2\pi}{\tau}t\right)\right) \qquad (24)$$

Triangular heat flux:

$$Q(z,t) = \begin{cases} 4f(z)\left(\dfrac{t}{\tau} - k\right) & 0 \leq \dfrac{t}{k\tau} < \dfrac{1}{2} \\[2mm] 4f(z)\left(1 + k - \dfrac{t}{\tau}\right) & \dfrac{1}{2} \leq \dfrac{t}{k\tau} < 1 \end{cases} \qquad (25)$$

Square heat flux:

$$Q(z,t) = \begin{cases} 2f(z) & 0 \leq \dfrac{t}{k\tau} < \dfrac{1}{2} \\[2mm] 0 & \dfrac{1}{2} \leq \dfrac{t}{k\tau} < 1 \end{cases} \qquad (26)$$

Where: $f(z) = \dfrac{4Q_0 z(L-z)}{L^2}$, $Q_0 = 12000\ W/m^2$,

$\tau = 60 s$ (period), k=1,2,...,n (number of achieved periods)
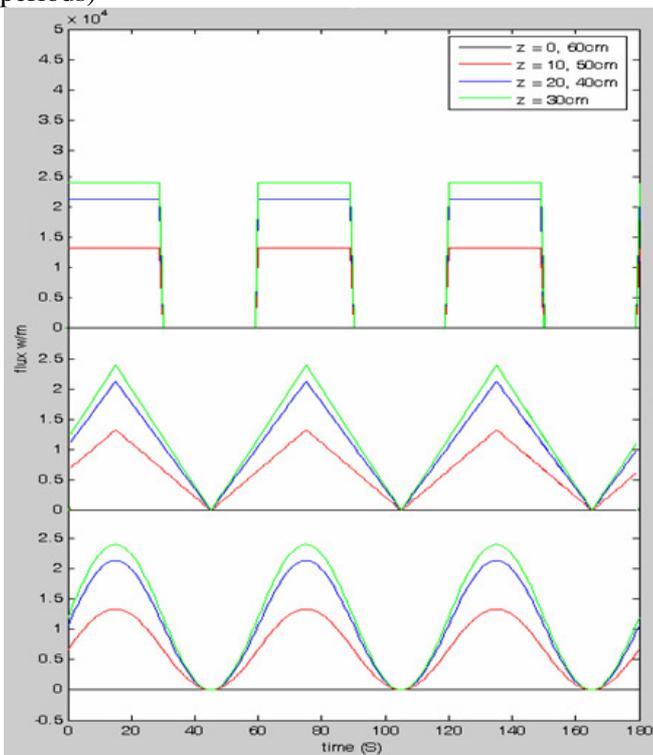
Fig. 4: Variation of the applied heat flux (sinusoidal, triangular, and square).

For the mechanical problem:

$V = 0$ at $z = 0$ and $z = L$

$U = V = \sigma_{rr} = \sigma_{zz} = \sigma_{rz} = 0$ at $t = 0$

In these conditions, the distribution of the temperature, for the sinusoidal case, is presented in Fig. 5 at time $t = 9000\ s$. This distribution clearly depends on the variation of the heat flux as well as on the thermal sources resulting from the plastic and elastic deformation. The maximum of the temperature corresponds to the maximum of the heat flux.
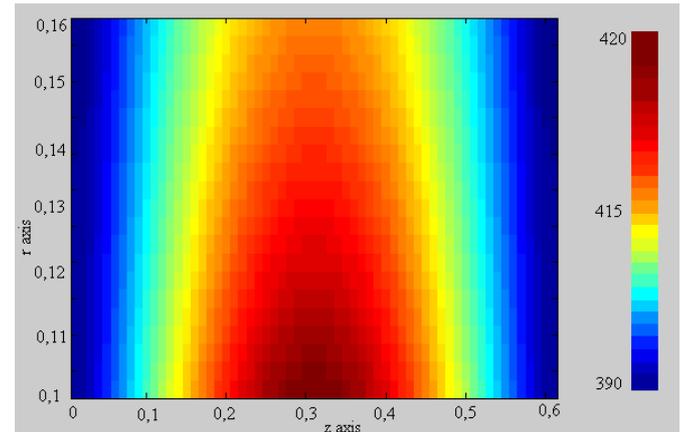
Fig. 5: Distribution of the temperature at time 9000s

5.2 Numerical results and discussion

In this study, we take into consideration the plastic regime in addition to the elastic regime. In fact, the thermal heat balance formulation takes into account the effect of the plastic and elastic deformations in the thermal sources (see eq. 9). This effect was not studied previously in [14].

In this last work, we did a comparison between the limits of damage by considering various percentages of thickness of these two materials, but this work did not cover the study of the influence of the thermal load (period, shape and amplitude of heat flux) with the thickness on the damage.

The evolutions of the temperature and the stresses, at three positions (r=R1, R2 and R3), are presented respectively on figures 6 and 7 for different forms of the heat flux (for $\tau = 60s$ and for $e_1 = e_2 = 0.03$ m.).

We can see clearly that the temperature and stress do not follow exactly the shape of the heat flux applied especially for the triangular and square excitations cases. Their shapes are all almost the same.

In figures 8 and 9, we present respectively, for different periods of the heat flux applied, the average temperature and stress of compression at the quasi-steady state. We can observe the same

behavior for the three heat fluxes applied for any value of the period.
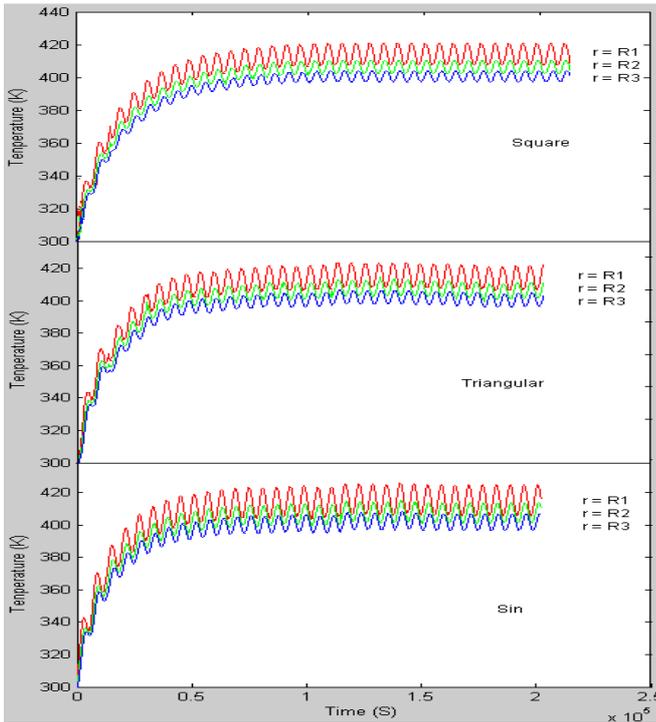

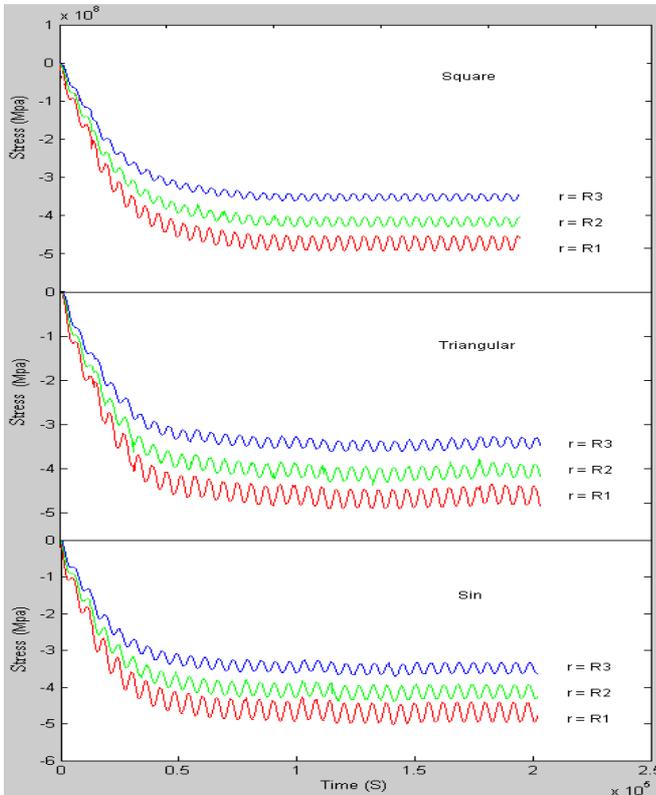**Fig. 6:** Evolution of the temperature under different forms of the heat flux ($e_1 = e_2 = 0.03$ m, $\tau = 60s$).

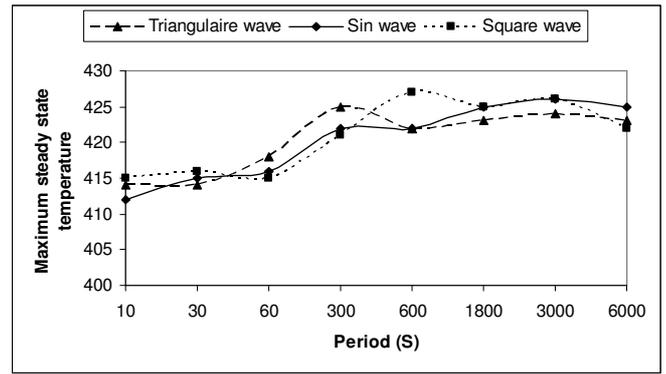**Fig. 7:** Evolution of stress under different forms of the heat flux ($e_1 = e_2 = 0.03$ m, $\tau = 60s$).

Fig. 8: Variation of the maximum average temperature at steady state, for $z = L/2$, $r = R_1$, $e_1 = e_2 = 0.03$ m
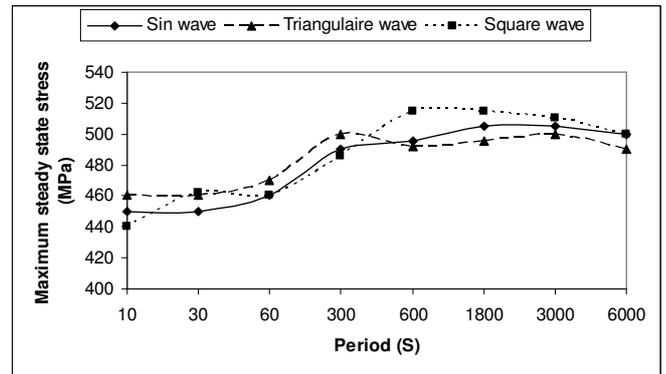

Fig. 9: Variation of the maximum average stress at steady state, for $z = L/2$, $r = R_1$, $e_1 = e_2 = 0.03$ m.

For these three shapes, figures 10, 11 and 12 show the damage obtained for a particular period $\tau = 6000\ s$. For the other values of the period, the results are presented in figure 13 for the damage and in figure 14 for the lifetime of the multi-material. Theses curves have the same shape for the three cases of the heat fluxes analyzed.
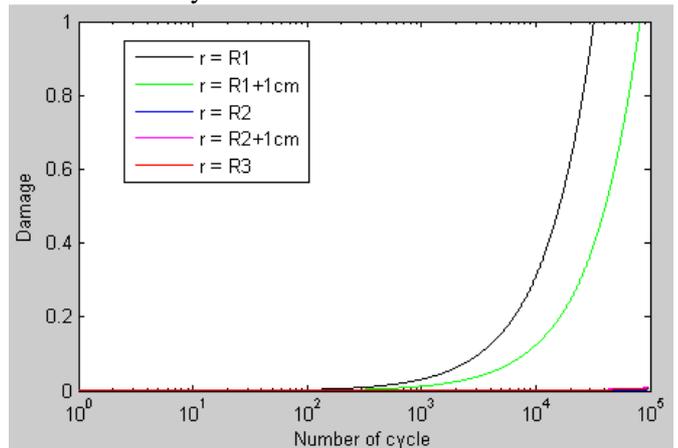
Fig. 10: Evolution of damage at period $\tau = 6000s$ for the sinusoidal heat flux case, $e_1 = e_2 = 0.03$ m.
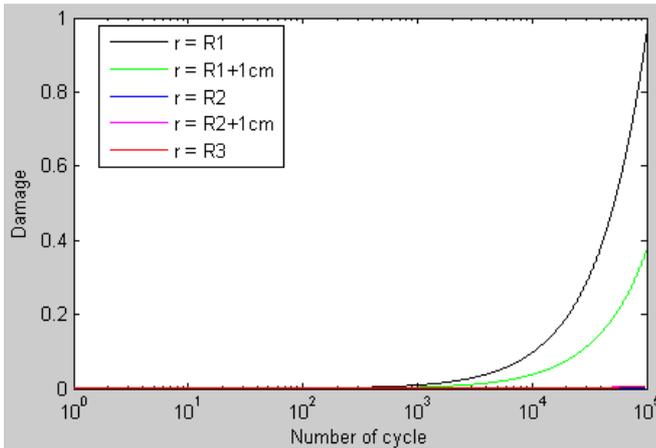
Fig. 11: Evolution of the damage at period $\tau = 6000 s$ for triangular wave heat flux, ($e_1 = e_2 = 0.03$ m).
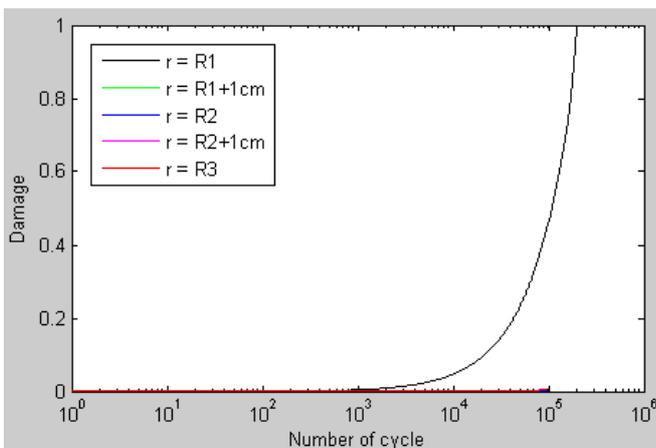

Fig. 12: Evolution of the damage at period $\tau = 6000 s$ for square wave heat flux, ($e_1 = e_2 = 0.03$ m).
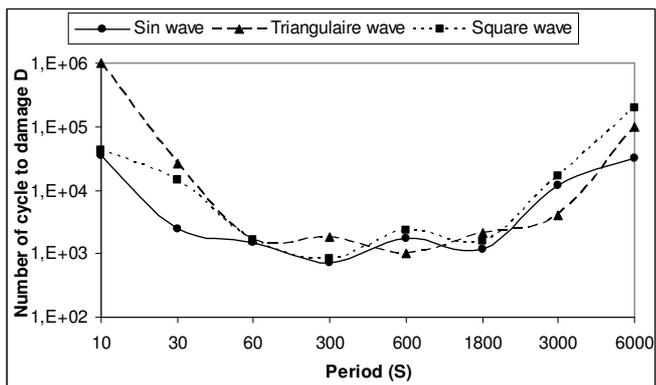

Fig. 13: Variation of the number of cycles to obtain the damage in function of the period of heat fluxes, $e_1 = e_2 = 0.03 \text{m}$
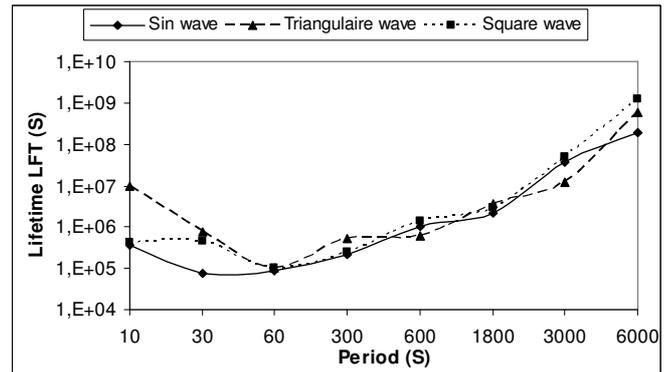

Fig. 14: Variation of the time to obtain the damage (lifetime) function of the period heat fluxes, $e_1 = e_2 = 0.03 \text{m}$

- Influence of the total thickness ($e = e_1 + e_2$) of the multi-material

The simulated computations, figures 15 to 20, are obtained in the conditions described before and for the sinusoidal heat flux case. We can conclude the following remarks:

- While the total thickness of the body increases, the lifetime and the number of cycles to damage increases, Figs. 19 and 20. This effect can be explain by the fact that the maximum applied temperature and the stress at $z=L/2$, and $r=R_1$ (critical point) decrease when the total thickness increases, figures 17 and 18.

- Figs. 15 and 16 represent the amplitude of the temperature and the stress in the multi-material at $r = R_1$ and $r = R_3$. We can conclude that, when the thickness increases, the amplitude of the temperature and the stress at $r = R_1$ increases. As the total thickness of the multi-material increases, the influence of the convective heat transfer condition (cooling face $r = R_3$) decreases and then the temperature and the stress amplitudes decrease as well.

Fig. 19 shows that the number of cycles to damage is a function of both the solicitation period and the thickness. We can remark that when the period decreases, the number of cycles to damage increases starting from a certain value of the period *(300 s)*, [23]. After this value, the number of cycles to damage becomes more and more stable with a slight increase accompanying the increase of the period. This is caused by the relaxation effect at high periods. The maximum amplitude of the temperature and the stress become also more stable when the period of the thermal load solicitation reaches high values.

This figure shows also that the domains of using a high number of cycles to damage can be obtained for the heat flux periods: $\tau < 30$ and $\tau > 2400$.

Fig. 20 shows the lifetime of the material defined as the result of the multiplication between the numbers of cycles to damage, fig. 19, and the period at each point: $LFT = D \times \tau$.

For the small thicknesses ($e = 0.02$ m and $e = 0.04$ m), the lifetime increases when the period increases, despite the increasing values of the temperature and the stress figs. 17 and 18.

For the lower periods (high frequency), the multi-material is operating under hard conditions, i.e. the multi-material is subjected to a faster damage corresponding to a weak lifetime, although the temperature and the stress are relatively low, [14], [23].

For high thicknesses, ($e = 0.06$ m, $e = 0.08$ m in fig. 20), the lifetime is high in the domain of periods $\tau < 30$ and $\tau > 2400$. In fact, for the lower periods, the temperature and the stress amplitudes of the oscillations, figs. 15 and 16, under thermal cycling heat flux, are weak and not sufficient to damage the multi-material, contrarily to the case of higher periods.
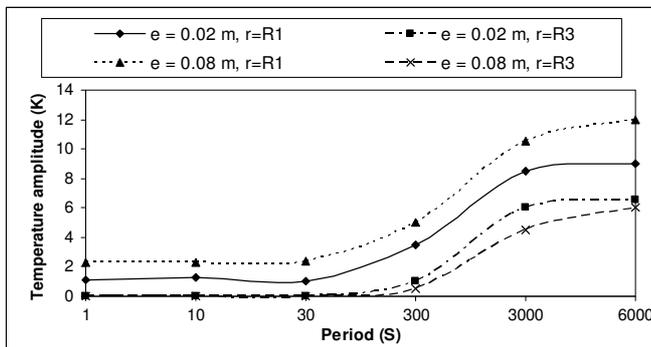

Fig. 15: Variation of the maximum amplitude of the temperature at $z = 0.5\,L$, for different periods of heat flux, ($e_1 = e_2$)

So, we can observe, for this geometry and for this thermal heat flux solicitation, a minimum value of lifetime corresponding to a particular period, for example $\tau = 30$ s for $e = 0.08$ m and $\tau = 60$ s for $e = 0.06$ m, figs 14 and 20.
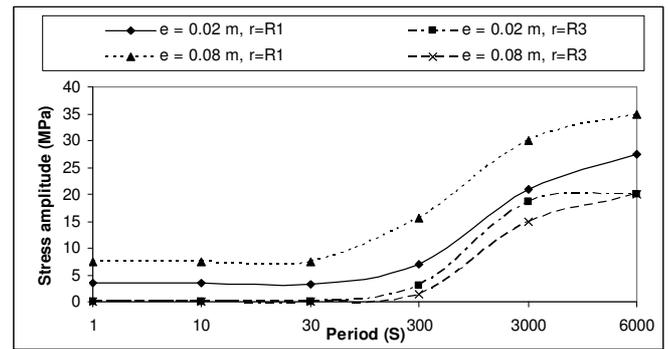

Fig. 16: Variation of the maximum amplitude of the stress at $z = 0.5\,L$, for different periods of heat flux, ($e_1 = e_2$)
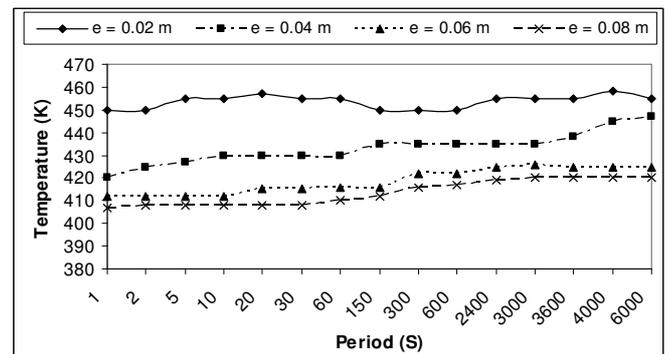

Fig. 17: Variation of the average steady state temperature at $z = 0.5\,L$, and $r = R_1$, for different periods of heat flux (sinusoidal case), and different thicknesses, ($e_1 = e_2$).
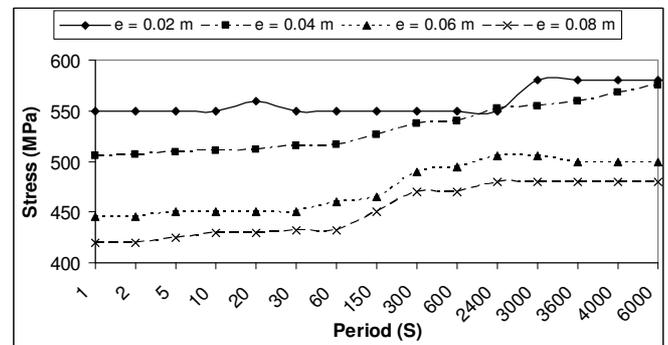

Fig. 18: Variation of the average steady state stress at $z = 0.5\,L$, and $r = R_1$, for different periods of heat flux (sinusoidal case), and different thicknesses, ($e_1 = e_2$).
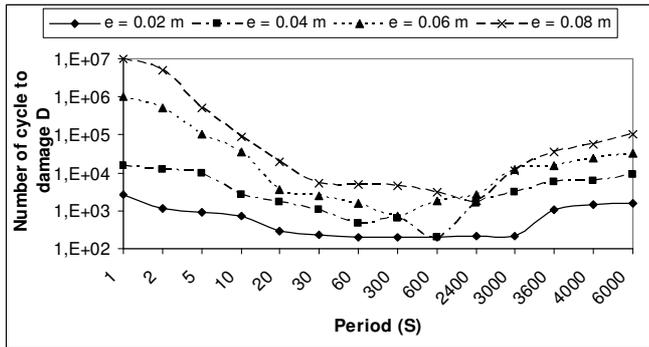
Fig. 19: Variation of the number of cycles to damage in function of the period for sinusoidal heat flux and different thicknesses
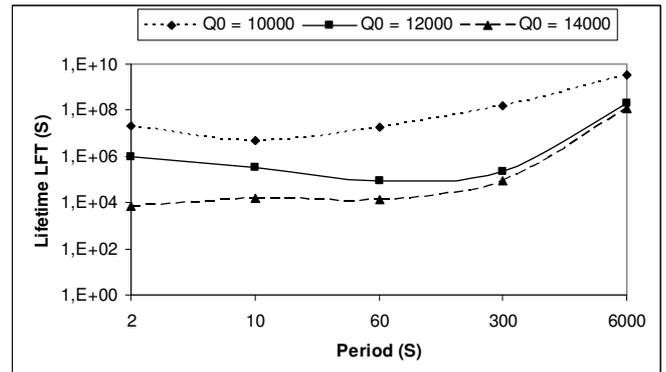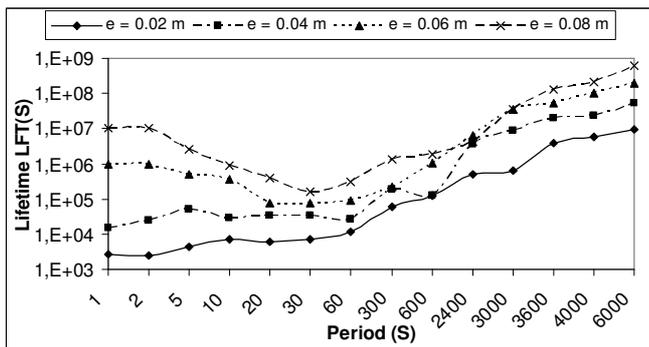

Fig. 20: Variation of the lifetime function of the period for different thicknesses.

Influence of the amplitude of the heat flux:

The effect of the amplitude (*A=2xQ0*) of the heat flux on the damage is presented in figs 21 and 22. The results obtained are very obvious; when the amplitude increases, the number of cycles to damage and the lifetime decrease.
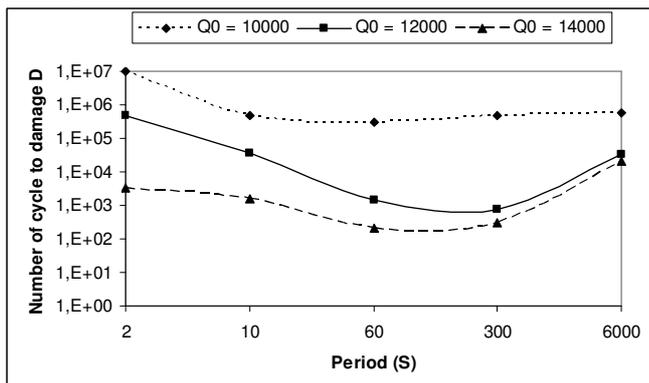

Fig. 21: Variation of the number of cycles to damage in function of the period for different amplitudes of the heat flux

Fig. 22: Variation of the lifetime function of the period for different amplitudes of the heat flux.

6 Conclusions

In this work, a numerical study, of the damage of multi-materials in thermo-elasto-plastic regime, is presented. The damage model is applied on the equivalent (or homogenization) material. The damage, represented by the number of cycles and the lifetime is presented for different shapes of the heat flux applied and for different thicknesses of the multi-material. The main results are summarized as follows:

- The numerical results show that the three shapes of the heat flux; sinusoidal, triangular and square, have the same results on the damage.

- The period of the thermal load has a remarkable influence on the damage. We demonstrate that around a range of periods, there is a hard influence on the lifetime of the multi-material. This depends also on the geometrical properties of the material studied.

- Minimum values or range of periods for which the lifetime of the material is relatively low exist indeed.

- The amplitude of the heat flux applied has also a direct influence on the damage. If the amplitude increases, the lifetime as well as the number of cycles to damage decreases.

References:

[1] Dentsoras, A. J.; Kouvaritakis, E. P., Effects of vibration frequency on fatigue crack propagation of a polymer at resonance, *Elsevier*, 1995, Vol. 50, No. 4, pp. 467-473.

[2] Primdahl, K.; Kustom, R., Cooling the APS Storage Ring Radio-Frequency Accelerating Cavities thermal stress/fatigue Analysis and Cavity Cooling Configuration, 1996, *IEEE* 0-7803-3053-6/9.

[3] Singh, N.; Khelawan, R.; Mathur, G. N., Effect of stress ratio and frequency on fatigue crack growth rate of 2618 aluminium alloy silicon carbide metal matrix composite, *Defence Materials & Stores*

Research & Development Establishment, 2001, India Vol. 24, No. 2pp. 169–171.

[4] Wang, R. J.; Shang, D. G.; Li, L. S.; Li, C. S., Fatigue damage model based on the natural frequency changes for spot-welded joints, 2007, *Elsevier*, pp. 1047-1055.

[5] Boulaajaj, A.; Cabrera, J.M.; Prado, J.M., Effect of initial microstructure, frequency and temperature on the low cycle fatigue behaviour of the soldering alloys 96.5Sn–3.5Ag and 63Sn–37Pb, 2007, *Elsevier*, pp. 220-228.

[6] Lemaitre, J.; Chaboche, J.L., Mécanique des matériaux solides, 1988*, DUNOD, second edition, BORDAS*, Paris.

[7] Saanouni K.; Chaboche, J.L., Computational damage mechanics. Application to metal forming. Numerical and Computational methods, 2003*, Elsevier*, vol. 3, n. 7, p. 321-376 Oxford.

[8] Vidal, E., Prévision de la durée de vie en fatigue multiaxiale sous sollicitations d'amplitude variable à l'aide d'un critère global, 1996, *PhD Thesis*, INSA de Lyon.

[9] Jabbado, M., Fatique polycyclique des structures metalliques: durée de vie sous chargement variables, 2006, PhD Thesis, Ecole Polytechnique.

[10] Jaskea, C.E.; Deevib, S.C.; Shademana, S.S. Fatigue and cyclic deformation behavior of iron aluminide, aCC Technologies, Dublin, OH 43016-8761, USA, 1998*, Research, Development and Engineering Center, Philip Morris USA, Richmond*, VA 23234.

[11] Charkaluk, E.; Bignonnet, A.; Thomas, J. Dimensionnement à la fatigue thermomécanique de structures dans l'industrie automobile, 2004, *J. Mécanique & Industries*, 5, 27-40.

[12] Abboudi, S.; Bonnet, P., Approche locale de l'endommagement sous des conditions thermiques variables, 1996, *C.R. 10émes Journ. Nat. Comp. (JNC10)*, pp 597-605.

[13] Abboudi, S.; Bonnet P., Transient Thermomechanical Homogenization of Multilayer Material, 1997, *Second International Symposium on Thermal Stresses and Related Topics, Rochester*, pp. 455-458.

[14] Sheffler, K. D.; Alexander, J. A., Vaccum thermal-mechanical fatigue testing of tow iron base high temperature alloys, 1972, t*opical report no.3 for national aeronautics and space administration, Nasa, under contract nas-3-6010*.

[15] Taher, B.; Youness, R.; Abboudi, S., Numerical analysis of thermomechanical behavior of a multimaterial under thermal cycling conditions, 2006, *PVP2006 – ICPVT – 11, ASME Pressure Vessels and Piping Division Conference*, Vancouver, Canada, ASME digital store PVP2006-ICPVT-11-93495,10p., in CD-ROM.

[16] Taher, B.; Abboudi, S.; Younes, R., Study of homogenization technique in a tow-layer cylindrical material, 2007, *IMECE 2007, International Mechanical Engineering Congress and Exposition*, ASME digital store IMECE2007-44084, Seattle, Washington, USA, 10p., in CD-ROM.

[17] Hetnarski Richard B. (1986): Thermal stresses I, Elsevier, Rochester institute of technology, New York, USA.

[18] Hetnarski Richard B., *Thermal stresses IV*, 1999, Lastran, Rochester institute of technology, New York, USA.

[19] Hetnarski Richard B., *Thermal stresses V*, 1999, Lastran, Rochester institute of technology, New York, USA.

[20] Bonnet, P., Contribution à l'étude des couplages thermiques et mécaniques dans les multimateriaux sous sollicitations thermiques variables, 1998, PhD Thesis, University of Technology of Belfort-Montbéliard, UTBM.

[21] Reddy, B.V.; Deevi, S.C., Thermophysical properties of FeAl (Fe-40 at.%Al), 2000*, Research Development and Engineering Center*, 4201 Commerce Road, Philip Morris USA, Richmond, VA 23234.

[22] Masahashi, N.; Watanabe, S.; Hanada, S. , Microstructure and Oxidation Behavior of Low Pressure Plasma Sprayed Iron Aluminides, 2001, *Institute for Materials Research, Tohoku University*, Katahira, Aoba, Sendai 980-8577 Japan.

[23] Kawasaki, N.; Kobayashi, S.; Hasebe, S., Spectra Thermal Fatigue Tests under Frequency Controlled Fluid Temperature Variation -Transient Temperature Measurement Tests, 2006, *Proceedings of 2006 ASME Pressure Vessels and Piping Division Conference (PVP2006)* Vancouver, Canada, ICPV11-93548, 8p., in CD-ROM.

[24] Allix, O.; Bahlouli, N.; Cluzel, C.; Perret, L. (): Modélisation et identification du comportement mécanique en température du pli élémentaire d'un stratifié carbone-epoxy, C.R. 1994, *9émes Journ. Nat. Comp. (JNC9)*, pp 475-484.

[25] Raud, C., Fissuration des composites carbone à matrice thermostable en traction isotherme et cyclage thermique, 1993, PhD thesis, university of Paris 6.

[26] E. S. gaddis D. Brian Spalding J. Taborek, Heat exchanger design handbook Physical properties tome 5, 1989.